

Supplementary Information

The Telomere Length Landscape of Prostate Cancer

Julie Livingstone^{1,2,3,4}, Yu-Jia Shiah⁵, Takafumi N. Yamaguchi^{1,2,3,4}, Lawrence E. Heisler⁵, Vincent Huang⁵, Robert Lesurf⁵, Tsumugi Gebo^{1,2,3,4}, Benjamin Carlin^{1,2,3,4}, Stefan Eng^{1,2,3,4}, Erik Drysdale⁵, Jeffrey Green⁵, Theodorus van der Kwast^{6,7}, Robert G. Bristow^{6,8,9}, Michael Fraser⁶, Paul C. Boutros^{*,1,2,3,4,8,10}

¹ Department of Human Genetics, University of California, Los Angeles, CA 90095, USA

² Department of Urology, University of California, Los Angeles, CA 90024, USA

³ Jonsson Comprehensive Cancer Centre, University of California, Los Angeles, CA 90024, USA

⁴ Institute for Precision Health, University of California, Los Angeles, CA 90024, USA

⁵ Ontario Institute for Cancer Research, Toronto, ON M5G 0A3, Canada

⁶ Princess Margaret Cancer Centre, University Health Network, Toronto, ON M5G 2M9, Canada

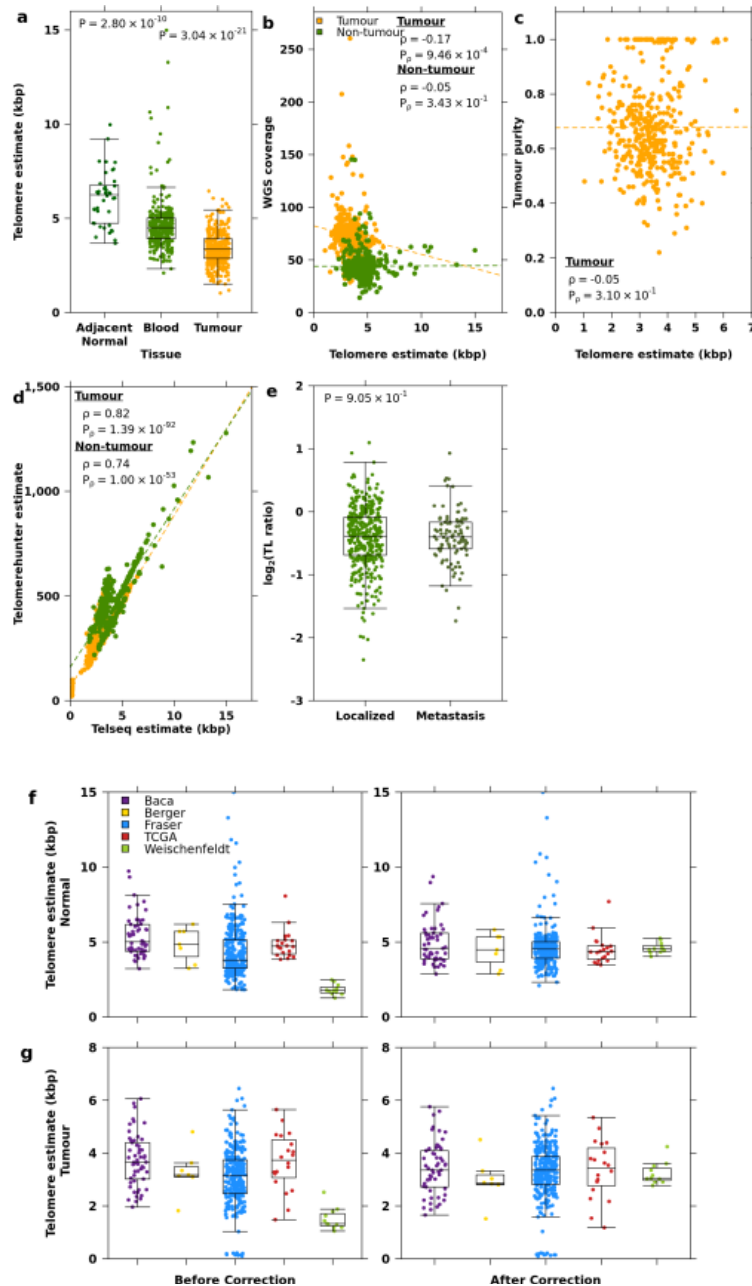
⁷ Department of Pathology, Laboratory Medicine Program, University Health Network, Toronto, ON M5G 2C4, Canada

⁸ Department of Medical Biophysics, University of Toronto, Toronto, ON M5G 1L7, Canada

⁹ Manchester Cancer Research Centre, Manchester, United Kingdom

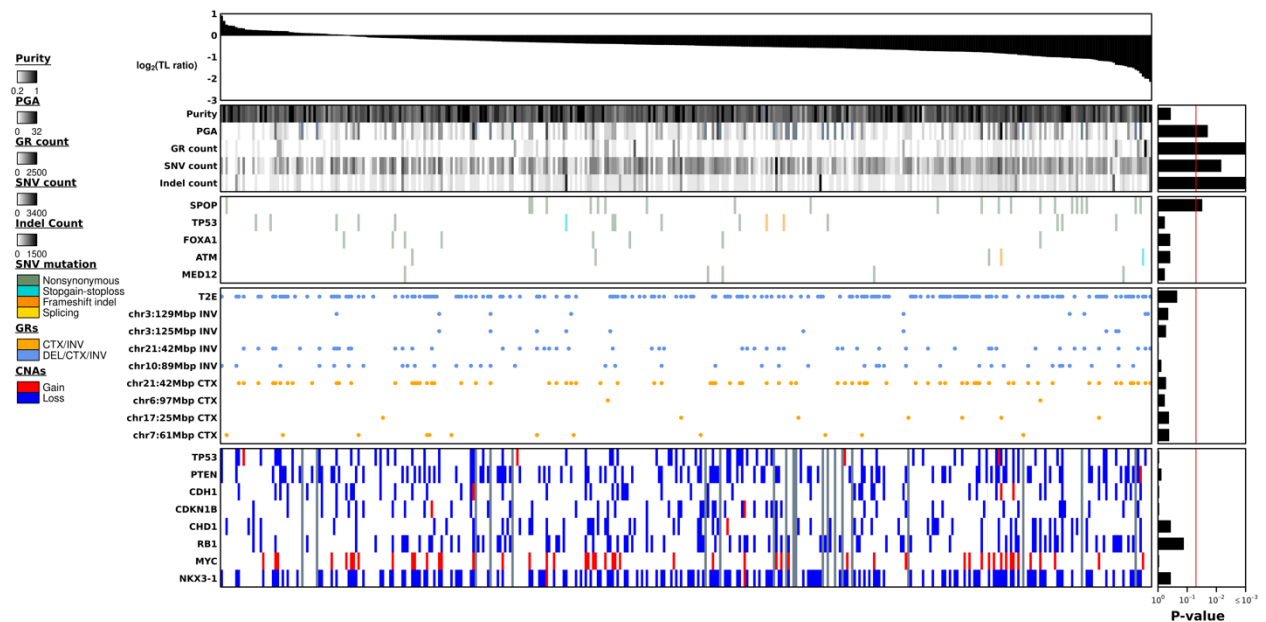
¹⁰ Department of Pharmacology and Toxicology, University of Toronto, Toronto, ON M5S 1A8, Canada

*Corresponding Author

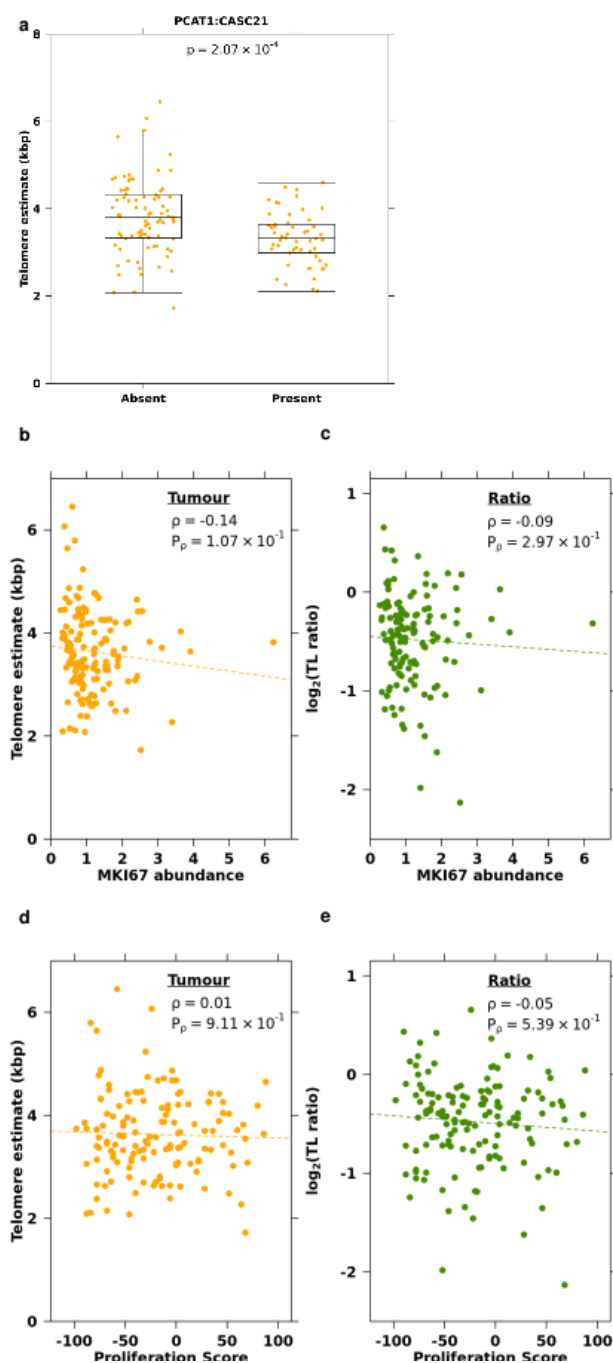


Supplementary Figure 1 | Telomere length is independent of technical variables.

a, Comparison of telomere length (TL) in adjacent, histologically normal prostate tissue ($n = 40$), blood ($n = 341$), and tumour tissue ($n = 381$). P values are from a two-sided Mann Whitney U-test comparing adjacent normal TL to blood TL and tumour TL. **b**, Two-sided Spearman's correlation of telomere length ($n = 381$) estimated by TelSeq and WGS coverage **c**, tumour purity and **d**, TelomereHunter estimates. **e**, Comparison of TL ratio in localized ($n = 381$) and metastatic ($n = 101$) prostate cancer samples. P value is from a two-sided Mann-Whitney U test. **f**, Non-tumour TL and **g**, tumour TL were batch corrected using a linear model (see Methods). Pre-corrected values and corrected values are shown. Box plots depict the upper and lower quartiles, with the median shown as a solid line; whiskers indicate 1.5 times the interquartile range (IQR).

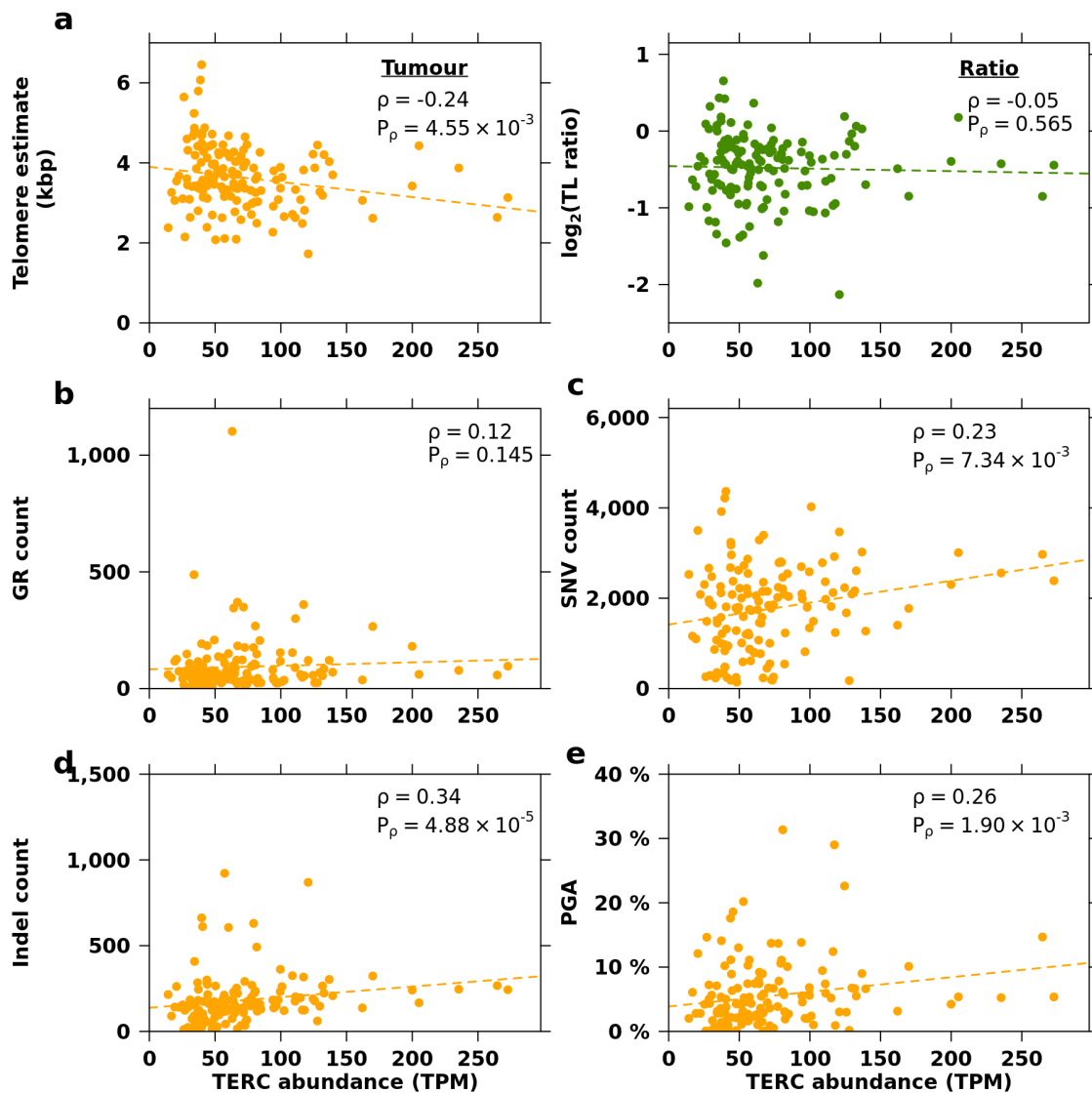


Supplementary Figure 2 | Genomic associations with telomere length (TL) ratio. TL ratio (tumour TL / non-tumour TL) is ranked in descending order. The association of TL ratio and measures of mutational burden, TMPRSS2:ERG (T2E) fusion status, as well as, known prostate cancer genes with recurrent copy number aberrations (CNAs), coding single-nucleotide variants (SNVs), and genomic rearrangements (GRs) are shown. Bar plots indicate the statistical significance of each association (see Methods).



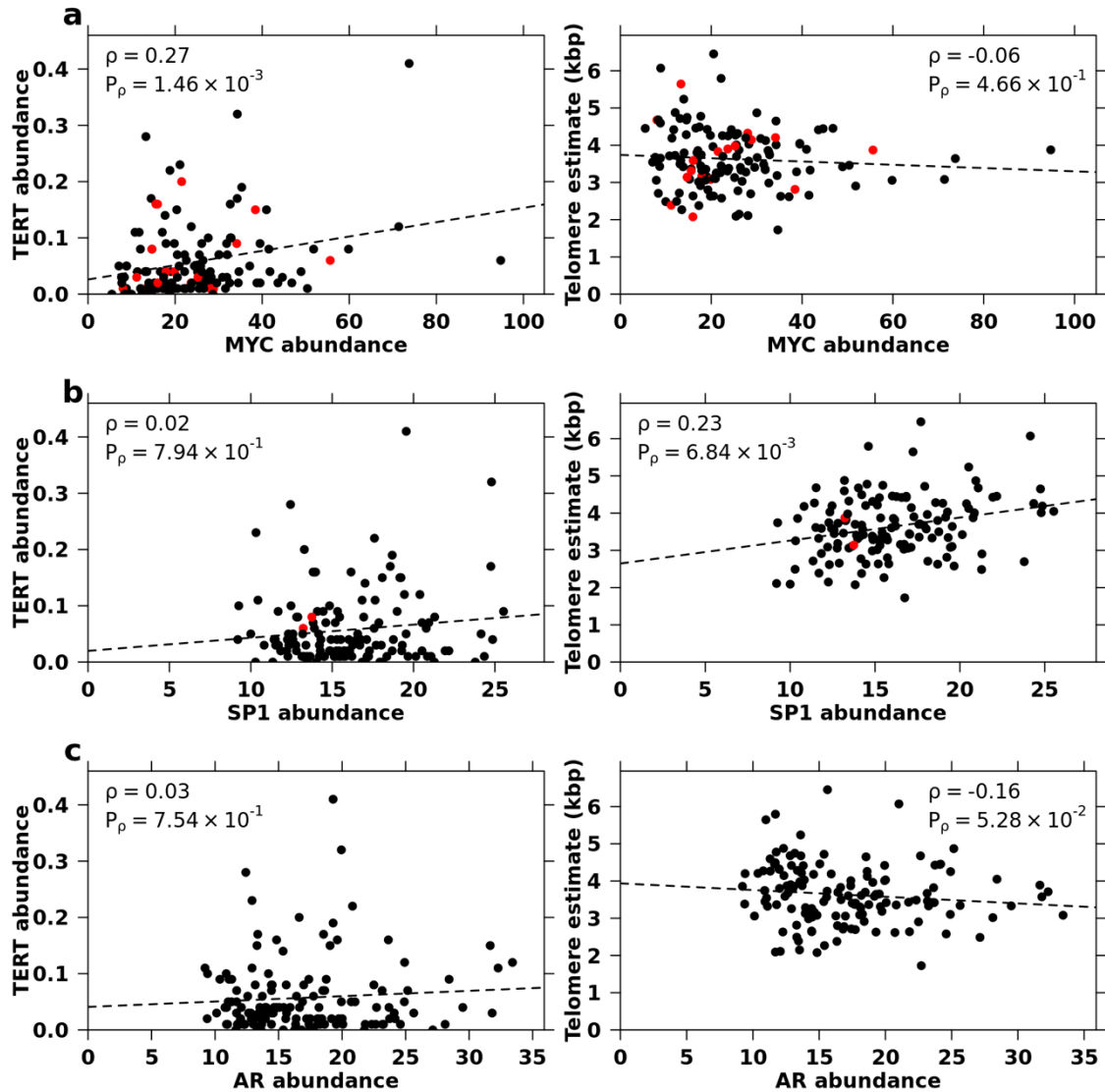
Supplementary Figure 3 | Fusions are association with tumour TL and TL ratio.

a, Difference in tumour TL between samples with a PCAT1:CASC21 gene fusion and those without. Box plots depict the upper and lower quartiles, with the median shown as a solid line; whiskers indicate 1.5 times the interquartile range (IQR). **b-c**, Correlation of MKI57 RNA abundance with **b**, tumour TL and **c**, TL ratio. **d-e**, Correlation of proliferation scores with **d**, tumour TL and **e**, TL ratio. Two-sided Spearman's ρ and P values are displayed.



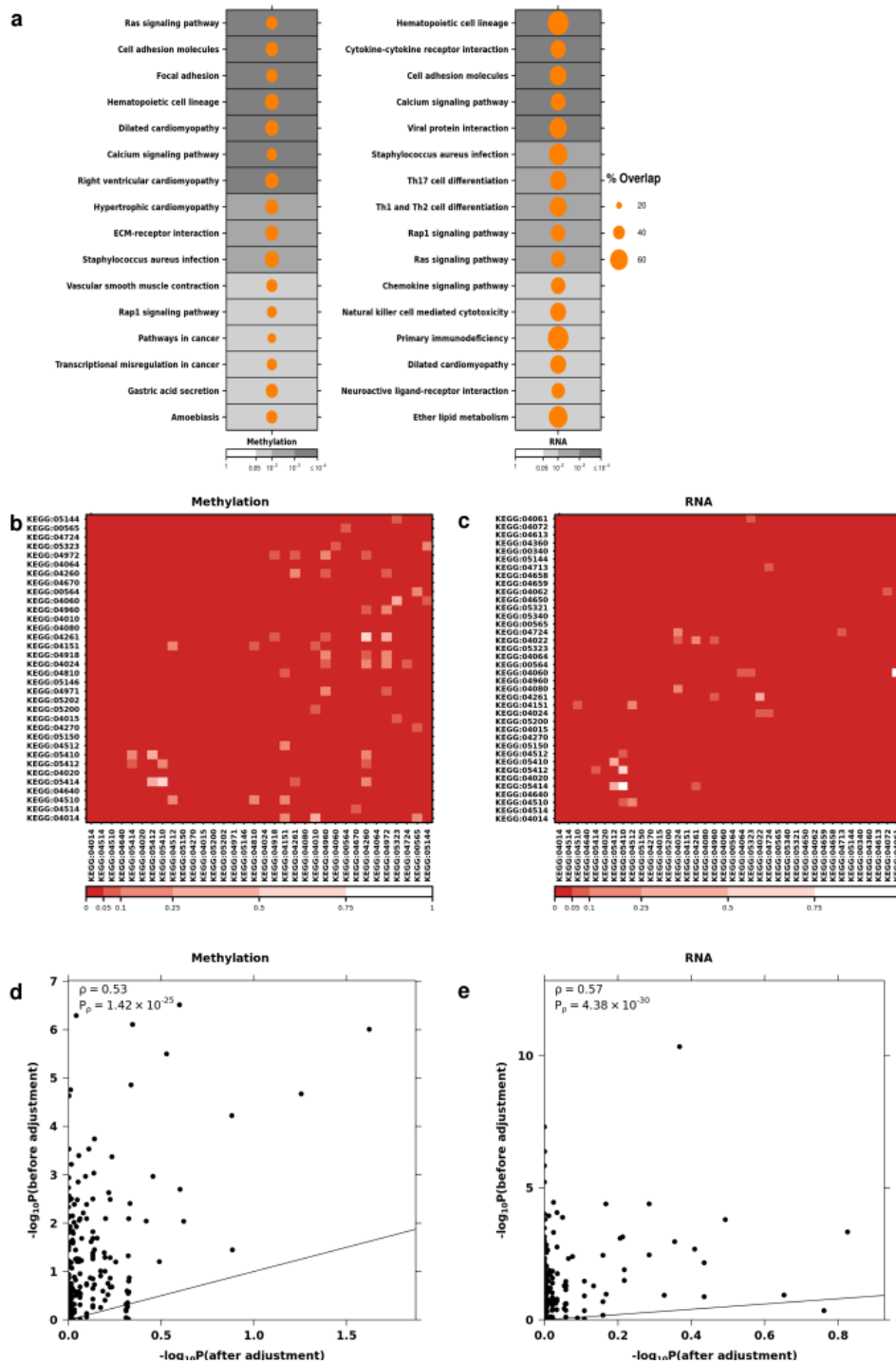
Supplementary Figure 4 | Genomic correlates of TERC abundance.

a, Correlation of *TERC* abundance with tumour TL and TL ratio. **b-e**, Correlation of *TERC* abundance and the **b**, number of genomic rearrangements (GRs), **c**, number of single-nucleotide variants (SNVs), **d**, number of indels and **e**, percent genome altered (PGA). Two-sided Spearman's ρ and P values are displayed ($n = 139$).

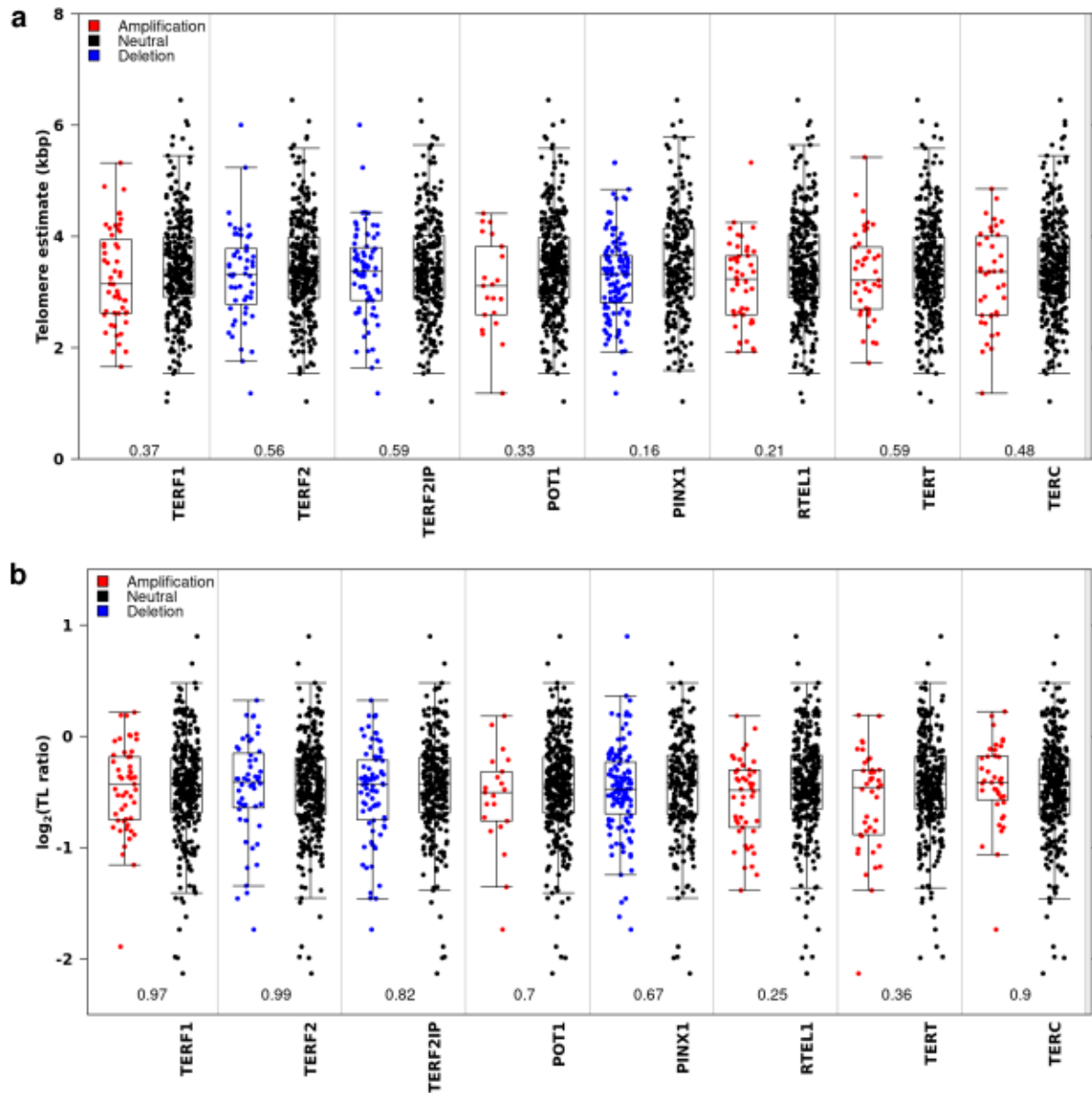


Supplementary Figure 5 | Transcription factors of *TERT* are correlated with *TERT* abundance and telomere length (TL).

a-c, Correlation of *TERT* transcription factors **a**, *MYC*, **b**, *SP1* and **c**, *AR* with *TERT* abundance and tumour TL. Two-sided Spearman's ρ and P values are displayed. Red dots indicate an amplification in that sample for the displayed transcription factor.

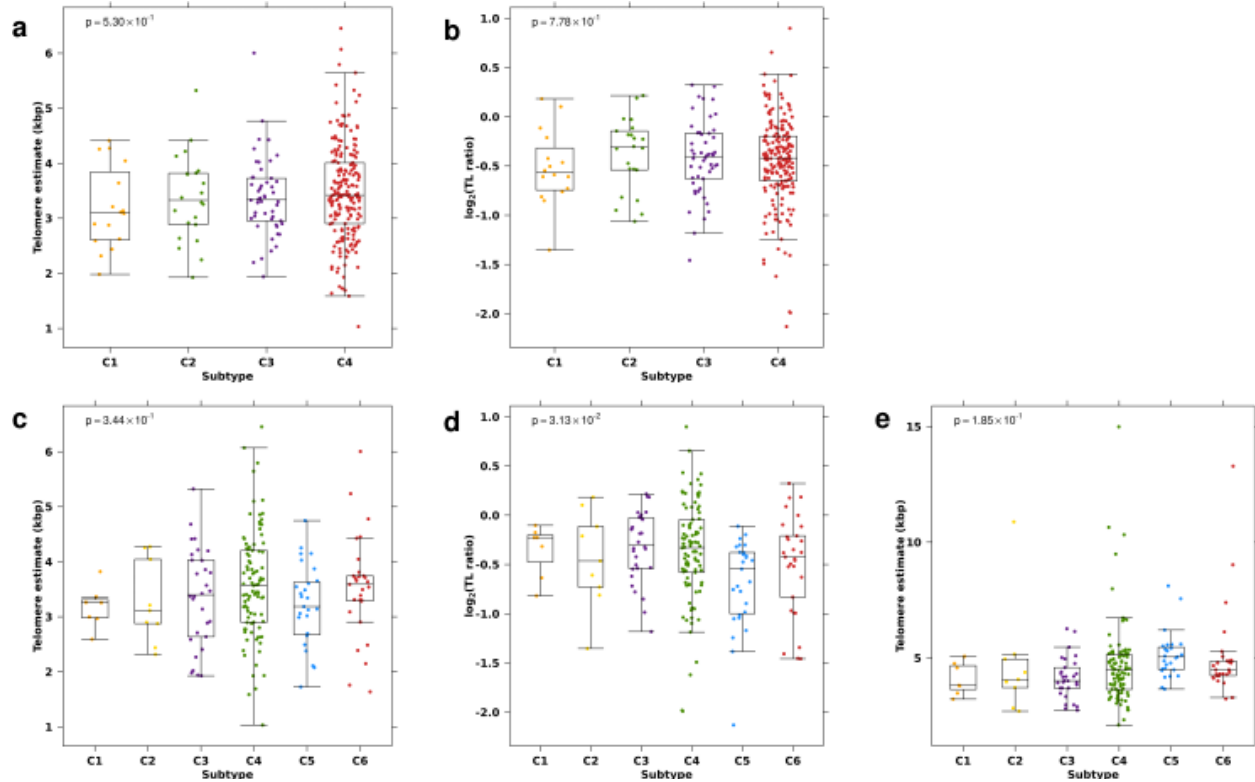


Supplementary Figure 6 | Pathways enriched in genes with methylation or transcriptomic profiles that are correlated with tumour TL. **a**, Dotmap representing enriched pathways. Size of dot indicates the percentage of overlap between correlated genes and genes in the pathway. Background colour indicates unadjusted P values from gprofiler2. **b-c**, Heatmaps of crosstalk matrices where white indicates loss of significance after removal of intersecting genes. **d-e**, Comparison of P values from an one-sided Fisher's Exact test before and after crosstalk adjustment.



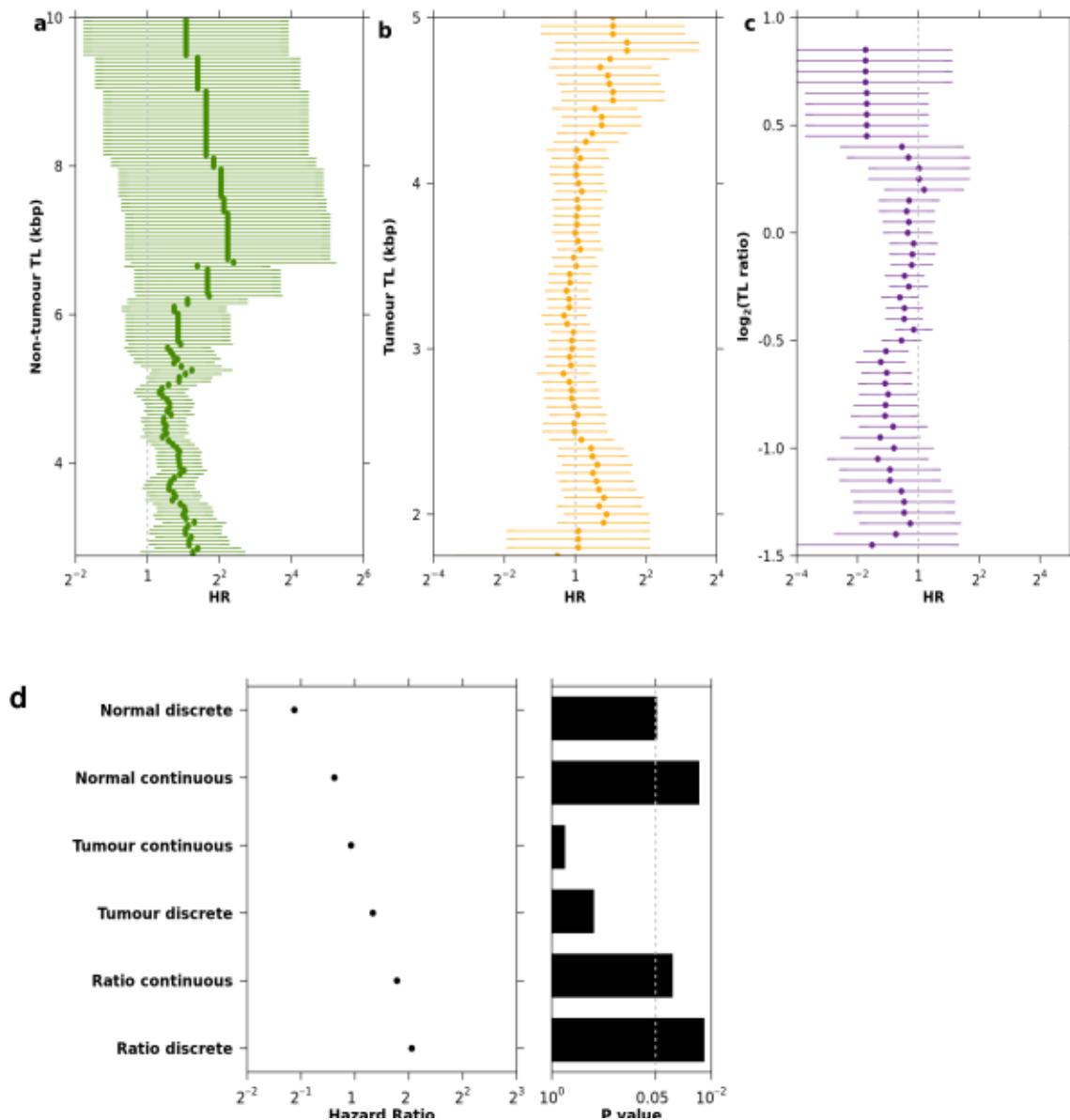
Supplementary Figure 7 | Telomere length (TL) does not differ by copy number status in genes that make up the telomere complex.

a-b, Difference in **a**, tumour TL and **b**, TL ratio between samples ($n = 381$) with a copy number aberration and those without in telomere complex genes. Q values are from a two-sided Mann-Whitney U test. Box plots depict the upper and lower quartiles, with the median shown as a solid line; whiskers indicate 1.5 times the interquartile range (IQR).



Supplementary Figure 8 | Association of telomere length (TL) with CNA subtypes.

a-b, Association of **a**, tumour TL and **b**, TL ratio with four previously identified copy number aberration subtypes¹. *P* value is from a two-way ANOVA ($n = 284$). **c-e**, Association of **c**, tumour TL and **d**, TL ratio and **e**, non-tumour TL with seven previously identified CNA subtypes². *P* value is from a two-way ANOVA ($n = 196$). Box plots depict the upper and lower quartiles, with the median shown as a solid line; whiskers indicate 1.5 times the interquartile range (IQR).



Supplementary Figure 9 | Telomere length (TL) is associated with biochemical relapse.

a-c, Association of **a**, non-tumour TL, **b**, tumour TL and **c**, TL ratio with biochemical relapse using a Cox proportional hazards model ($n = 290$) at different TL cutoffs, incremented by 50 bp. Error bars represent the 95% confidence interval (HR = hazard ratio). **d**, Comparison of the best dichotomized Cox proportional hazards models and models fit with TL as a continuous value.

Supplementary References

1. Lalonde, E. *et al.* Tumour genomic and microenvironmental heterogeneity for integrated prediction of 5-year biochemical recurrence of prostate cancer: a retrospective cohort study. *Lancet Oncol.* **15**, 1521–1532 (2014).
2. Fraser, M. *et al.* Genomic hallmarks of localized, non-indolent prostate cancer. *Nature* **541**, 359–364 (2017).